

A Liquid Water Model: Density Variation from Supercooled to Superheated States, Prediction of H-Bonds, and Temperature Limits

Arshad Khan*

Chemistry Department, Pennsylvania State University, DuBois, Pennsylvania 15801

Received: May 3, 2000; In Final Form: August 1, 2000

The expressions for density and fraction of H-bonding H atoms are derived and applied from supercooled to superheated states of liquid water (H₂O). The anomalous density variation (around 4 °C) with temperature is explained solely on the basis of H-bonding and non-H-bonding (NHB) H atoms in the liquid. Interesting structural changes are postulated as the temperature of liquid water increases from a very low to a very high value. The limits of supercooling and superheating temperatures are calculated to be around 180 and 980 K, respectively, at 1 atm pressure.

1. Introduction

Water is an unusual liquid with quite a few anomalous properties. These include temperature variation of density, heat capacity at constant pressure (C_P), coefficients of expansion, compressibility, etc. For many years, efforts have been made to explain the anomalous properties of liquid water at the molecular level. Almost all these models assume certain structural features for liquid water. Nemethy and Scheraga¹ interpreted the X-ray diffraction results of Morgan and Warren² by considering a "mixture model" that depicts liquid water to be made up of a number of distinguishable H-bonded species. The interstitial model (a special type of mixture model) of Pauling³ and Samoilov⁴ assumes the presence of bulky species with a number of non-H-bonded water molecules within their cage cavities. Pople's model⁵ considers a majority of H-bonds in the liquid as distorted rather than broken. The Bernal model,⁶ an extension of the distorted H-bond model, assumes each water molecule to be bonded to four other molecules and form a random network of four-, five-, six-, and seven-membered rings instead of an ordered structure. These earlier models, however, fail to account for all the peaks in the experimental radial distribution functions.⁷ The simulation studies^{8–14} are more successful in this regard and explain all the peaks of the radial distribution functions, especially near ambient temperatures.¹⁵ It predicts the presence of non-H-bonding H (NHB H) atoms and an increase in their number as the temperature is increased. However, the position of the density maximum at around 4 °C has not yet been accurately predicted by these simulation studies.

Among the most recent versions of mixture models of liquid water, the model due to Benson and Siebert,¹⁶ Robinson and co-workers,¹⁷ Khan et al.,¹⁸ and Weinhold¹⁹ deserve to be mentioned. The Benson-Siebert model assumes the existence of polymeric H-bonded octamers in equilibrium with cyclic tetramers in the liquid. Even though this model reproduces the heat capacity values within 2%, the experimentally observed trend²⁰ cannot be reproduced. Also, the assumption of isolated cubic clusters (even at room temperature) in this model¹⁶ is inconsistent with simulation results reported so far. Robinson and co-workers¹⁷ put forward a model that considers a mixture of open structure of low density (like ice Ih) and a dense compact structure (like ice-II, III, V, and VI²¹) of high density in the liquid and describes different properties of liquid water.

One of the drawbacks of this model is that it introduces a large number (11) of adjustable parameters. Khan et al.'s model¹⁸ is based on the assumption of a mixture of NHB H and HB H atoms in the liquid water and explains the anomalous density variation with temperature. This model, however, requires heat capacity values for the calculation of NHB H or HB H atoms. The Weinhold model¹⁹ assumes the existence of equilibria between molecular clusters and describes a method for calculating equilibrium properties of liquids. As mentioned before, the presence of disconnected clusters, especially at ambient temperatures, is inconsistent with the vast amount of simulation results reported so far. Even though the derivation of the density expression in Khan et al.'s model¹⁸ involves the consideration of clusters (which can be interconnected to each other), the final density expression does not include any structure parameter of the cluster. This observation suggests that the assumption of cluster formation in the liquid water cannot be a requirement for the derivation of a density expression. In addition, there is also a motivation to extend density calculations to supercooled and superheated states when an increasing number of researchers are trying to understand the properties of liquid water in these regions. Several experimental results as well as theoretical predictions are reported at these extreme conditions and have initiated an intense debate regarding the accuracy of some of these results. For example, the stability-limit conjecture, put forward by Speedy and Angell,^{22–24} suggests a supercooling limit of –45 °C and draws an analogy with the reported limit (known at that time) of superheating^{24–26} temperature of around 315 (± 10) °C. At these limiting temperatures, singularities in thermodynamic properties are postulated. There is a strong disagreement among the researchers regarding the existence as well as the magnitude of such temperature limits and various properties prevailing at these temperatures. For example, the supercooling temperature limit, as reported by researchers, ranges from no temperature limit to –73 to –45 °C.^{17,27–29} Undoubtedly, additional studies are required to resolve the above controversy, and hence, to achieve a better understanding of liquid water under these extreme conditions.

In the superheated region, there is also a persistent debate over the presence or absence of intact H-bonds at a supercritical temperature of 400 °C or higher (higher than the above limit). On the basis of neutron diffraction studies and OH pair

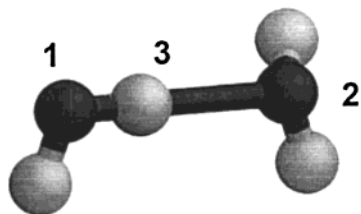


Figure 1. A water dimer is shown to illustrate H-bonding and to aid in the derivation of H-bonding expression for liquid water.

correlation function, Postorino et al.³⁰ (see also ref 31) suggest that almost all the H-bonds in the liquid water are broken at a temperature (T) of 400 °C (673 K). One of the concerns, as recognized by the authors, is that the thermal energy (kT , where k is the Boltzmann's constant) at 400 °C is considerably less than the energy of an H-bond. The above finding of Postorino et al.³⁰ has been challenged and criticized by many on the basis of both experimental and theoretical considerations.^{32–35} All these studies suggest that significant H-bonds exist even at temperatures much higher than 400 °C. It is generally believed³⁶ that certain corrections applied to neutron scattering data can be a significant source of error in the estimation of H-bonds, and hence, these estimates can be unreliable. By recognizing the problem of data analysis, Soper et al.³⁷ have applied a new method of analysis and obtained a small (but nonzero) number of H-bonds at 400 °C. This result, even though it suggests the presence of a small number of H-bonds at extreme temperatures, is not as significant as those from other studies. A comparison of H-bond estimates from different studies is discussed below.

The purpose of this paper is to predict the anomalous density variation of liquid water on the basis of a model that incorporates only two adjustable parameters and to determine the temperature limits of supercooling and superheating at a constant pressure (1 atm). In the first part of this paper, we derive expressions for the fraction of H-bonds [$F(T)$] and density, followed by discussions of structural changes with temperature and limits of supercooling and superheating temperatures.

2. Deriving $F(T)$, the Fraction H-Bonded in Liquid H_2O

An H-bond is defined³⁸ in terms of a cutoff O–O distance (3.10 Å) and an O–H–O angle (146°). When the O–O distance is longer or the O–H–O angle is smaller than the cutoff value, the H–O bond can be considered to be a broken bond. Figure 1 shows an H-bond between two water molecules with an $O_1H_3O_2$ angle of 180°. The H_3 – O_2 in the figure represents an H-bond that binds two water molecules together. There are five modes that can contribute to H-bond breaking. These include three degrees of translational motion (along three perpendicular directions) of molecule 1 (represented by O_1) relative to molecule 2 (represented by O_2) and two degrees of rotational motion of molecule 1 around an axis perpendicular to the O_1 – H_3 – O_2 axis. The rotation of molecule 1 around the O_1 – H_3 – O_2 axis cannot lead to a bond dissociation for which this rotational motion is not considered as a bond-breaking mode. Let us assume that an overall energy E (kcal/mol) remains distributed among the above five active modes with an average value of $E/5$ per active mode. When a fast energy transfer among the five active modes is considered, the minimum E value may correspond to an actual H-bond breaking energy. This assumption of fast energy transfer is in line with the common belief of fast structural changes in liquid water. The fraction of total number of water molecules with energy of $E/5$ or larger in an active mode is given by $\exp[-E \times 1000/(5RT)]$, where R is 1.987 cal K^{−1} mol^{−1} and T is the temperature in K. The above

fraction of molecules will cause bond breaking and give rise to NHB H atoms in the liquid. That is,

$$1 - F(T) = \exp[-E \times 1000/(5RT)] = \exp[-E \times 100.65425/T],$$

or,

$$F(T) = 1 - \exp[-E \times 100.65425/T] \quad (1)$$

where, $F(T)$ represents the fraction of intact H-bonds.

3. Expressions for the Density of Liquid H_2O

This part of the derivation is very similar to what we have already reported.¹⁸ In brief, there are two major factors that determine the density variation with temperature: the H-bond breaking and the thermal expansion of the liquid volume. Since H-bonds can enclose ring structures with cavities, the bond breaking will allow water molecules to approach more closely to each other, and thus, can increase the density. The thermal expansion of volume is a well-known property of a liquid and can decrease the liquid density. Hence, the interplay of above two factors is responsible for an anomalous variation of density of liquid water with temperature.

3.1. Density Increase due to H-Bond Breaking. The increase in density (relative to ice at 273 K with no NHB H atoms) caused by H-bond breaking can be considered to be proportional to the number of NHB H atoms in the liquid and is given by

$$\Delta\rho_1(T) = \alpha[1 - F(T)] \quad (2a)$$

By applying eq 1 and the density value of ice at 273 K, the following expression can be derived:

$$\rho(T) - 0.9165 = \alpha \exp[-E \times 100.65425/T] \quad (2b)$$

Here, α is a proportionality constant, and the following expression for α can be derived from the liquid water (0.99989 g/mL) and the solid hexagonal ice density (0.9165 g/mL) at 273 K:

$$\alpha = 0.08339 \exp[E \times 0.368697] \quad (3)$$

3.2. Thermal Expansion and Decrease in Density. Assuming a linear relationship of volume with temperature, the following expression can be written:

$$V(T) = V(T_0) [1 + \beta(T - T_0)] \quad (4)$$

where, β is the thermal coefficient of volume expansion, $V(T_0)$ is the volume of liquid water at T_0 (273 K) and $(T - T_0)$ is the temperature change. The density (for a unit mass) will be given by

$$\rho(T) = 1/V(T) \approx \rho(T_0) - \beta(T - T_0)/V(T_0) = \rho(T_0) - \beta_1(T - T_0)/V(T) \quad (5)$$

where, β_1 is the thermal coefficient of volume expansion at T_0 (273 K) and is given by $\Delta V/[V(T_0)\Delta T]$.

Since the volume of liquid water decreases when H-bonds are broken, the volume can be expressed as an inverse function of fraction of broken bonds (NHB H atoms), i.e.,

$$V(T) \propto 1/[1 - F(T)] = \beta_2/[1 - F(T)] \quad (6)$$

Now the eq 5 can be written as

$$\Delta\rho_2(T) = \rho(T) - \rho(273) = -\gamma(T - 273)[1 - F(T)] \quad (7)$$

where, γ is given by β_1/β_2 . It should be noticed that the volume expression (eq 6) not only depends on fraction of broken bonds or $F(T)$ values, it also depends on β_2 . Thus β_2 , and hence, γ incorporates other effects (like H-bond distortion or oxygen atom rearrangements, etc.) that may change the volume or density of the liquid.

3.3. Calculated Density and Comparison with Experiments. The net density change from H-bond breaking and volume expansion is given by

$$\Delta\rho_{\text{net}}(T) = \Delta\rho_1(T) + \Delta\rho_2(T) \quad (8)$$

By applying eqs 2a, 2b, 3, and 7, the following expression can be written:

$$\rho(T) = 0.9165 + [\alpha - \gamma(T - 273)][1 - F(T)] \quad (9a)$$

or,

$$\rho(T) = 0.9165 + [0.08339 \exp(E \times 0.368697) - \gamma(T - 273)] \exp(-E \times 100.65425/T) \quad (9b)$$

There are only two parameters, E and γ , in the expression (eq 9b), and they are evaluated by using experimental density values³⁹ from 274 to 280 K (Table 1). The E and γ values, thus obtained, are 5.6095 kcal/mol and 0.004738, respectively. The aim is to examine the predicted density values beyond the above temperature range. Indeed, as presented in Table 1 and Figure 2, an excellent agreement can be noticed with Kell's experimental results,³⁹ especially within the temperature range of around 263 to 373 K (−10 to 100 °C). In the supercooled region (below 273 K), the maximum error of about 1% is noticed at 243 K (−30 °C), and in the superheated region (above 373 K) the maximum error of about 1.5% is noticed at 423 K (150 °C, maximum temperature at which experimental data is available). It should be pointed out that a number of experimental results are reported for the supercooled region (below 273 K), and these results vary significantly from one experiment to another.^{39–42} Two such experimental results^{39,40} are presented in Table 1 and Figure 2 for a comparison. Some of the experimental values are derived by a linear interpolation of the reported data. In Figure 2, the dashed curve represents data from Kell's experiment,³⁹ filled circles with a solid curve represents experimental data from Schuffle and Venugopalan,⁴⁰ and the solid curve represents our calculated results. Even though our calculated values (Table 1) are in better agreement with those reported by Schuffle and Venugopalan⁴⁰ (maximum deviation of around 0.60%) in the supercooled region, a small but systematic deviation from the experimental results can be noticed at lower temperatures (below 270 K). Similarly, in the superheated region, a systematic deviation from the experimental results are noticed at higher temperatures (above 370 K). These deviations can be traced back to the fact that E and γ values have been held fixed from supercooled to superheated region, and it is likely that they change with temperature. To test this hypothesis, we varied E and γ so as to get a best fit to Kell's experimental results in the supercooled region. This provides E and γ values of around 16.13 kcal/mol and 0.7455, respectively. The calculated density values on the basis of these values are presented in Table 2. The maximum deviation is now around 0.07% when compared with experimental results of ref 39. Similarly, in superheated region, an E value of around 4.0864 kcal/mol and γ of 0.0025 give density values (Table 3) in much better agreement with the experiment.³⁹ The maximum deviation in this region is now less than 0.007%. Overall, a good agreement between the predicted density values and the experimental

TABLE 1: Calculated and Experimental^{39,40} Density Values, ρ (g/mL), Together with Calculated $F(T)$ Values (Fraction H-Bonded)^a

temp (K)	ρ (g/mL) expt ³⁹	ρ (g/mL) expt ⁴⁰	ρ (g/mL) calc	$F(T)$ calc
243	0.9838540	0.9891196	0.9950213	0.9020736
248	0.9895850	0.9929092	0.9963561	0.8973770
253	0.9935470	0.9960052	0.9974881	0.8926542
258	0.9962830	0.9974143	0.9984123	0.8879096
263	0.9981170	0.9988601	0.9991240	0.8831477
268	0.9992560	0.9994282	0.9996191	0.8783724
271	0.9996660		0.9998108	0.8755024
273	0.9998395	0.9997006	0.9998943	0.8735875
274	0.9998985		0.9999227	0.8726297
275	0.9999399		0.9999421	0.8716717
276	0.9999642		0.9999526	0.8707135
277	0.9999720		0.9999541	0.8697552
278	0.9999638		0.9999466	0.8687967
279	0.9999402		0.9999301	0.8678381
280	0.9999015		0.9999046	0.8668794
281	0.9998482		0.9998700	0.8659207
282	0.9997808		0.9998263	0.8649619
283	0.9996996		0.9997736	0.8640032
288	0.9990996		0.9993732	0.8592100
291	0.9985956		0.9990232	0.8563356
293	0.9982041		0.9987439	0.8544202
298	0.9970449		0.9978844	0.8496363
303	0.9956473		0.9967939	0.8448608
308	0.9940319		0.9954718	0.8400960
311	0.9929653		0.9945673	0.8372432
313	0.9922158		0.9939179	0.8353442
318	0.9902132		0.9921322	0.8306071
323	0.9880363		0.9901151	0.8258868
333	0.9831989		0.9853885	0.8165027
343	0.9777696		0.9797448	0.8072040
353	0.9717978		0.9731932	0.7980005
358	0.9686203		0.9695804	0.7934372
363	0.9653201		0.9657452	0.7889008
368	0.9619004		0.9616893	0.7843920
373	0.9583637		0.9574144	0.7799117
378	0.9547120		0.9529225	0.7754605
383	0.9509470		0.9482157	0.7710390
393	0.9430830		0.9381651	0.7622872
403	0.9347750		0.9272798	0.7536599
413	0.9260260		0.9155775	0.7451598
423	0.9168290		0.9030762	0.7367889
500			0.7820723	0.6767212
647			0.4517396	0.5821672

^a Density values of ref 40 are obtained by linear interpolation of reported values. $E = 5.6095$ kcal/mol and $\gamma = 0.004738$.

results suggests the validity of the liquid structure model presented here.

4. Significance of E Values

The present study suggests that the E value changes with temperature. In the intermediate temperature range (273–373 K), the E value of around 5.65 kcal/mol can explain the experimental results quite well with an error of less than 0.1%. The energy per active mode can be as small as 1.13 (5.65/5) kcal/mol and still can cause H-bond breaking. A fast energy transfer among the active modes allows sufficient energy to concentrate in an active mode and thus, causes an H-bond dissociation. Indeed, at this temperature range, the average H-bond energy is estimated to be around 5.7 kcal/mol.¹⁶

As temperature is increased, the H-bonds become weaker, and a smaller amount of energy is sufficient for H-bond breaking (fast energy transfer is still expected among the five modes). This explains a smaller value of E (4.0864 kcal/mol) for the superheated region (373–980 K, Table 3). These results suggest that the H-bond energy ranges from about 5.6 to less than 4.1

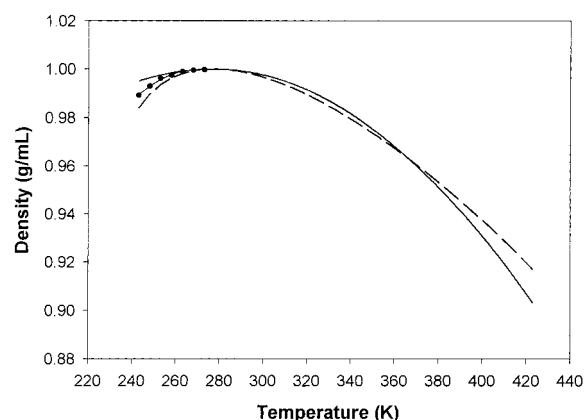


Figure 2. Kell's³⁹ (dashed curve) and Schuffe-Venugopalan's⁴⁰ experimental density values (filled circles with solid curve, supercooled region) together with our calculated values (solid curve, $E = 5.6095$ kcal/mol, $\gamma = 0.004738$) are presented. For a better description of supercooled and superheated regions, density values are also calculated with different E and γ values and presented in Tables 2 and 3, respectively.

TABLE 2: Calculated and Experimental³⁹ Density Values, ρ (g/mL), of Liquid H₂O Together with Calculated $F(T)$ Values for Supercooled Liquid Water, and Experimental Density Values for Supercooled Ordinary Ice⁵⁵ (Ice Ih)^a

temp (K)	ρ (g/mL) expt ³⁹	ρ (g/mL) calc	ρ (g/mL) ice hexagonal ⁵⁵	$F(T)$ calc
120		0.9166941		0.9999987
130		0.9170216		0.9999962
140		0.9177044		0.9999908
143		0.9180099	0.9324	0.9999883
145		0.9182455		0.9999863
150		0.9189611		0.9999801
153		0.9194879	0.9307	0.9999754
160		0.9210490		0.9999608
170		0.9242332		0.9999288
180		0.9287445	0.9271	0.9998790
190		0.9347352		0.9998055
200		0.9422340		0.9997018
213		0.9539959	0.9227	0.9995106
220		0.9610345		0.9993763
243	0.9838540	0.9845545	0.9193	0.9987458
248	0.9895850	0.9890215		0.9985650
253	0.9935470	0.9929534		0.9983668
258	0.9962830	0.9961871		0.9981505
263	0.9981170	0.9985475		0.9979155
268	0.9992560	0.9998477		0.9976610

^a $E = 16.13$ kcal/mol and $\gamma = 0.7455$.

kcal/mol within the temperature range of 273–980 K. As liquid water is cooled to lower temperatures (lower than 273 K), the H-bond energy is expected to approach that in solid ice (about 6.7 kcal/mol^{21b}). Since at such a low temperature range fast energy transfer among the five modes cannot be expected, the energy per mode is expected to be larger than 1.2 kcal/mol. Indeed, this value is around 3.2 kcal/mol (total of around 16 kcal/mol in five modes) as expected. Also, at this low temperature, it is not too likely to have too many modes with this amount of energy. This is why only a very small fraction of H-bonds is expected to break ($F(T)$ values almost 1.0, Table 2).

5. Significance of $F(T)$ Values

In addition to density values, Tables 1–3 provide fractions of H-bonds, $F(T)$, at different temperatures, and for three different energy values (E) as discussed above. Since the agreement (Figure 2, Table 1) between the experimental and the calculated density values is excellent within the normal

TABLE 3: Calculated and Experimental³⁹ Density Values, ρ (g/mL), Together with Calculated $F(T)$ Values for Superheated Liquid Water^a

temp (K)	ρ (g/mL) expt ³⁹	ρ (g/mL) calc	$F(T)$ calc
378	0.9547120	0.9546980	0.6631545
383	0.9509470	0.9509685	0.6583354
393	0.9430830	0.9431344	0.6488702
403	0.9347750	0.9348151	0.6396318
413	0.9260260	0.9260275	0.6306153
423	0.9168290	0.9167884	0.6218152
450		0.8897119	0.5990947
473		0.8643655	0.5808744
500		0.8321720	0.5607239
550		0.7663789	0.5266133
573		0.7337212	0.5121877
580		0.7235094	0.5079433
590		0.7087106	0.5019932
600		0.6936713	0.4961731
647		0.6199964	0.4704481
650		0.6151371	0.4688921
673		0.5773049	0.4572813
700		0.5316613	0.4443356
750		0.4439670	0.4221368
773		0.4023786	0.4126300
800		0.3526479	0.4019865
810		0.3339938	0.3981786
832		0.2925316	0.3900432
850		0.2581947	0.3836241
873		0.2138088	0.3757158
900		0.1610156	0.3668292
930		0.1015443	0.3574256
973		0.0149340	0.3447426
975		0.0108688	0.3441742
976		0.0088350	0.3438906
977		0.0068004	0.3436076
979		0.0027290	0.3430428
980		0.0006921	0.3427611
980		0.0002846	0.3427048
980		0.0000808	0.3426767

^a $E = 4.0864$ kcal/mol and $\gamma = 0.0025$.

temperature range (273 to 373 K), the $F(T)$ values within this temperature range, calculated at an E value of around 5.61 kcal/mol, can be considered to be fairly accurate. Similarly, the $F(T)$ values for $E = 16.13$ kcal/mol in supercooled region (Table 2), and $E = 4.0864$ kcal/mol for superheated region are expected to be quite reliable.

5.1. Comparison with other Reported Values. Some of our calculated percent of broken H-bonds, $[(1 - F(T)) \times 100]$, can be compared with those estimated on the basis of different experimental and theoretical results. These estimated values differ quite significantly from each other.^{21c} For example, for 273 K liquid water, estimates by Pauling⁴³ provides 15%, Haggis et al.⁴⁴ 9%, Ohmine⁴⁵ 10% and Khan et al.¹⁸ 13% of broken H-bond. The present calculation gives around 13% (Table 1) of broken bonds or about 87% of intact H-bonds at 273 K. Similarly, at 373 K our calculated value of about 22% broken bond (Table 1) is comparable to 20% of broken bond estimated by Haggis et al.⁴⁴ In the supercooled region, at 258 K (−15 °C) our calculated value of 99.8% intact H-bonds (Table 2) is comparable to Luck's^{46,47} estimate of more than 90% of intact bonds. From these comparisons, we observe that our calculated $F(T)$ values at different temperatures are in line with most other estimated values. Since our calculated $F(T)$ values are successfully applied for density calculation (eq 9b, providing excellent agreement with experiments), these $F(T)$ values (or eq 1) can be considered to be quite reliable.

5.2. H-Bonds in Supercooled and Superheated States. By referring to eq 1, we can postulate $F(T)$ values under two extreme situations. As T approaches 0 K, the $F(T)$ value

approaches 1. That is, there will be all intact H-bonds and no broken or NHB H bonds in the liquid at very low temperatures. Similarly, as T approaches ∞ , the $F(T)$ value approaches 0. That is, at a very high temperature, there will be no intact H-bonds, and only isolated water molecules will exist. As presented in Table 3, a significant percent of H-bonds exists at temperatures above 400 °C or even the critical point (374 °C or 647 K) and supports most of the previous experimental and simulation results.^{32–35} It should be noted that Gorbaty and Kalinichev⁴⁸ suggest that H-bonds in supercritical water can be observed at a temperature of 527 °C or even higher. This conclusion receives support from Yamanka et al.³² as well as Bellissent-Funel et al.³⁵ Indeed, the present study suggests (Table 3) the presence of about 40% intact H-bonds even at 527 °C (800 K) and about 34% intact H-bonds at around 707 °C (980 K).

At this point, we can compare our calculated values of H-bonds with those reported from neutron³⁷ and X-ray diffraction⁴⁸ studies for a supercritical temperature of 673 K. Because of differences in H-bond definitions, we present here the percent of H-bonds relative to that at ambient (298 K) i.e., $[F(T) \text{ at } 673 \text{ K}/F(T) \text{ at } 298 \text{ K}] \times 100$. In addition, a direct comparison of these results with ours is not possible as pressures applied in these experiments are significantly different from 1 atm (considered in our calculations). For example, Gorbaty-Kalinichev's⁴⁸ value of 55% is obtained under a pressure of around 1000 atm, Soper et al.'s value³⁷ of 42% is obtained under around 221 atm (with ambient at 1 atm), and our value of around 54% is obtained at 1 atm pressure. Since a higher pressure reduces the number of H-bonds in the liquid,⁴⁹ the experimental H-bond estimates at a higher pressure is expected to be lower than that at 1 atm. Hence, the result of Soper et al. is expected to be higher than 42% when the 673 K value is corrected for 1 atm pressure. Since both the 673 and 298 K values in Gorbaty-Kalinichev's⁴⁸ experiment are obtained at 1000 atm, a pressure correction to 1 atm is likely to increase both these values, and hence, the estimate of H-bond (relative to ambient) may remain close to 55%. Thus, a pressure-corrected experimental value becomes more in line with our H-bond value at 1 atm. It is to be mentioned that a certain amount of discrepancy may still exist between our calculated percent H-bond with those deduced from the X-ray and neutron diffraction pair distribution functions. One of the reasons may be because the above experimental data require a significant correction for an H-bond estimate, and thus, there may be errors introduced in H-bond estimates when corrections are applied, especially at higher temperatures.^{36,37} Our calculated H-bond values are expected to be reliable as they compare quite well with those deduced from other experimental or simulation studies (mentioned above)^{43–45} at relatively lower temperatures in which more reliable experimental or simulation results are expected. In addition, the anomalous experimental density variation is reproduced quite closely on the basis of these H-bond values.

5.3. Structural Changes with Temperature. By examining the effect of temperature on $F(T)$ values (Tables 1–3), we can arrive at an interesting conclusion regarding structural changes in liquid water. In the supercooled region (Table 2), especially at a temperature of 200 K or lower, the $F(T)$ value is very close to 1, indicating that almost all the H atoms in the liquid are H-bonded. The same is expected for an ice structure at a temperature of 273 K or lower. Thus, one may expect a predominant ice-like bonding in supercooled liquid water. As the temperature is increased, the $F(T)$ value is decreased as an increasing number of H-bonds break down. At around 373 K (Table 1), the $F(T)$ value becomes close to 0.75, suggesting

that about 75% of H-bonds are present in the liquid at this temperature. It is interesting to note that hollow cage clusters, such as cubic, dodecahedron, tetrakaidecahedron, pentakaidecahedron, hexakaidecahedron, etc. all have the same 75% of H-bonds.^{50–53} For example, $(\text{H}_2\text{O})_8$ cubic cage has four NHB H and 12 HB H atoms, $(\text{H}_2\text{O})_{20}$ dodecahedral cluster has 10 NHB H and 30 HB H atoms, $(\text{H}_2\text{O})_{24}$ tetrakaidecahedral cluster has 12 NHB H and 36 HB H atoms, etc. In general, in a hollow cage cluster with an even number of water molecules $(\text{H}_2\text{O})_x$, there are $x/2$ NHB H atoms and $(2x - x/2)$ HB H atoms giving 75% of H-bonding. While we cannot establish unambiguously that a hollow cluster formation takes place at around 373 K in liquid water, such a possibility cannot be totally ignored when one considers other possible structures with 75% of H-bonds. Among the alternative structures, one can consider structures with randomly ordered 75% of H-bonds and 25% of NHB H (non H-bonded or broken bonds) atoms. However, such a structure may be less favored over a spherical cluster when the minimization of free energy⁵⁰ is considered. Thus, there is a possibility of hollow cage formation at around 373 K from a highly interconnected ring structure of liquid water at lower temperatures. It is relevant to mention that the SPCE (the extended simple point charge model) simulation study of Guissani and Guillot⁵⁴ suggests a remarkable structural change within the temperature range of 423–473 K at which H-bonding per water molecule is decreased to around 3 (out of 4, 75% of H-bonding), and the liquid water expands at a higher rate on heating.

As the temperature is further increased to around 590 K (317 °C), the number of intact H-bonding atoms approaches 50% [$F(T)$ around 0.50, Table 3] with the remaining 50% of broken NHB H atoms. Again, among the ordered H-bonding structures, one can identify trigonal, tetragonal, pentagonal, etc., rings each of which has 50% of H-bonds and 50% of NHB H atoms. It is likely that such isolated ring structures may form at high temperatures from interconnected ring structures at lower temperatures. Even though a ring structure with externally bonded water molecules will also have 50% H-bonds, a single H-bond connecting an externally bonded H_2O molecule to the ring is more prone to dissociation than an H_2O molecule that forms part of the ring structure. Thus, disconnected ring structures are primarily expected at these high temperatures in liquid water. This will also represent a state in which liquid water will behave like a solvent of low polarity. Indeed the corresponding density is close to that of acetone at 20 °C (0.7899 g/mL).

5.4. Temperature Limits of Supercooling and Superheating. To determine a temperature limit for supercooling, we refer to Table 2 and Figure 3 and the calculated density values for liquid water and the experimental density values⁵⁵ for ordinary hexagonal ice (Ice Ih). As the temperature is lowered from, say, 243 K to around 180 K, the density of supercooled water is decreased from around 0.985 g/mL to around 0.929 g/mL. Within the same temperature range, the density of hexagonal ice is increased from around 0.919 g/mL to around 0.927 g/mL (an interpolated value from experimental data of ref 55). In other words, both the supercooled liquid water and ice will have the same density at around 180 K (−93 °C) and will be indistinguishable from each other. This is expected to be the lowest temperature limit for supercooled liquid water and is lower than the temperature limit estimated by Speedy and Angell²² (−45 °C) or Leyendekkers and Hunter²⁸ (−63 to −73 °C). Since the parameters used in present calculations are evaluated by using a number of experimental data points obtained under 1 atm

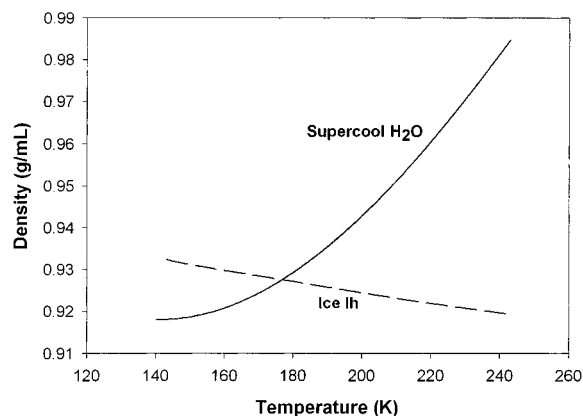


Figure 3. Temperature vs density curves are presented for supercooled H₂O (calculated) and ice Ih (ref 55). They intersect at around 180 K, a possible limit for supercooling at 1 atm.

pressure, the calculated density values refer to those under 1 atm pressure. Second, if other polymorphs of ice are stable at 1 atm pressure and have density values higher than that of the ordinary ice at supercooled temperatures, the liquid water may reach that density value at a higher temperature, and accordingly, the temperature limit of supercooling will be raised to a higher value (higher than 180 K).

In the superheated region also we arrive at the highest temperature limit on the basis of density values presented in Table 3. As the temperature is increased to around 980 K (707 °C), the density of liquid water approaches that of the H₂O gas at that temperature. The density of H₂O gas is calculated by assuming the validity of an ideal gas expression, $\rho(\text{gas}) = PM/RT$, where $P = 1$ atm, $M =$ molecular weight, and $R = 0.08206$ L atm/(K mol).

The density of H₂O gas (if water molecules remain unassociated), thus calculated, is around 0.000224 g/mL at 980 K and is very close to the liquid water (Table 3) value at around the same temperature. If water molecules remain associated as ring structures of, say, 3–6 H₂O molecules in the gas phase, the gas-phase density will be 3–6 times higher than 0.000224 g/mL, and that density is still close to that of the liquid water at around 980 K. On the basis of the above analysis, we can suggest that at around 980 K the liquid-phase water and gas-phase water will be indistinguishable, and hence, 980 K may represent the highest possible temperature for supercritical liquid water under 1 atm pressure. The $F(T)$ value at this temperature is about 0.34 (34% H-bonds), suggesting a very small amount of H-bonding in the liquid phase. This may represent disconnected ring structures together with isolated H₂O molecules in the liquid water.

6. Concluding Comments

The anomalous variation of density of liquid water from supercooled to superheated states has been explained solely on the basis of NHB and HB H atoms. The model predicts the presence of H-bonds at temperatures much higher than 400 °C and suggests structural changes from ice-like bonding (extensive H-bonding) in supercooled region ($F \approx 1$) to a hollow cluster type bonding at around 373 K ($F \approx 0.75$), ring-like bonding at around 590 K ($F \approx 0.50$), and rings and isolated water molecules ($F < 0.50$) at higher temperatures (1 atm).

One of the objectives of this paper is to establish major factors that determine the density variation of liquid water from supercooled to superheated states. The number of adjustable parameters in the final expression is kept to as few as possible

so that one can have a clear understanding of the physical significance of these parameters. In the process of doing so, a number of approximations were made that may account for certain deviations of calculated results from those of the experiment. For example, in deriving eq 5, the expansion of $1/V(T)$ has been carried out by assuming $1 + \beta(T - T_0) \ll 1$ and ignoring all the terms after the second one in the expansion series. At relatively lower temperatures, this is a fairly good approximation (β ranges from around 0.00015–0.00070 for 273–373 K). At higher temperatures, the value of $\beta(T - T_0)$ is expected to increase and the approximation may introduce an error in the calculated density values. However, the adjustment of γ (that incorporates β) for a good fit to the experimental data is expected to minimize this error. While the density change due to H-bond breaking is explicitly considered in this work, the density change caused by rearrangement of O atoms or H-bond distortions has been introduced in an indirect manner through the use of the γ parameter and a variable E . A distorted H-bond is expected to be a weaker bond that would require a smaller amount of energy for bond breaking. This is why the value of E is smaller for the superheated region. Similarly, for the same E and T values (eq 1), if the oxygen atom rearrangements or H-bond distortions change the volume $V(T)$, β_2 (eq 6) and hence (β_1/β_2) or γ will also change accordingly.

Even though there is no discontinuity in our density expression (eq 9b), practical limits will be reached when the density of liquid water becomes same as that of a solid ice polymorph (supercooling limit, 180 K) or gaseous H₂O (superheating limit, 980 K).

References and Notes

- (1) Nemethy, G.; Scheraga, H. A. *J. Chem. Phys.* **1962**, *36*, 3382.
- (2) Morgan, J.; Warren, B. E. *J. Chem. Phys.* **1938**, *6*, 666.
- (3) Pauling, L. In *Hydrogen Bonding*; Hadzi, Ed.; Pergamon Press: London, 1959.
- (4) Samoilov, Y. O. *Structure of Aqueous Electrolyte Solutions and the Hydration of Ions*, Consultants Bureau, New York, 1965.
- (5) Pople, J. A. *Proc. R. Soc. A* **1951**, *205*, 193.
- (6) Bernal, J. D. *Proc. R. Soc. A* **1964**, *280*, 299.
- (7) Narten, A. H.; Danford, M. D.; Levy, H. A. *Discuss. Faraday Soc.* **1967**, *43*, 97.
- (8) Stillinger, F. H.; Rahman, A. *J. Chem. Phys.* **1974**, *60*, 1545.
- (9) Jorgensen, W. L.; Madura, J. D. *Mol. Phys.* **1985**, *56*, 1381.
- (10) Ji, J.; Pettitt, B. M. *Mol. Phys.* **1994**, *82*, 67.
- (11) Billeter, S. R.; King, P. M.; van Gunsteren, W. F. *J. Chem. Phys.* **1994**, *100*, 6692.
- (12) Sciortino, F.; Sastry, S. *J. Chem. Phys.* **1994**, *100*, 3881.
- (13) Báez, L. A.; Clancy, P. *J. Chem. Phys.* **1994**, *101*, 9837.
- (14) Wallqvist, A.; Astrand, P. O. *J. Chem. Phys.* **1995**, *102*, 6559.
- (15) Chialvo, A. A.; Cummings, P. T. *J. Phys. Chem.* **1996**, *100*, 1309.
- (16) Benson, S. W.; Siebert, E. D. *J. Am. Chem. Soc.* **1992**, *114*, 4269.
- (17) Vedamuthu, M.; Singh, S.; Robinson, G. W. *J. Phys. Chem.* **1994**, *98*, 2222.
- (18) Khan, A.; Khan, R.; Khan, M. F.; Khanam, F. *Chem. Phys. Lett.* **1997**, *266*, 473.
- (19) Weinhold, F. *J. Chem. Phys.* **1998**, *109*, 367.
- (20) Weast, R. C., Ed. *CRC Handbook of Chemistry and Physics*, CRC Press: Boca Raton, FL, 1979; p D-174.
- (21) Eisenberg, D.; Kauzmann, W. *The Structure and Properties of Water*, Oxford University Press, 1969; (a) p 79, (b) p 139, (c) pp 178, 194.
- (22) Speedy, R. J.; Angell, C. A. *J. Chem. Phys.* **1976**, *65*, 851.
- (23) Speedy, R. J. *J. Phys. Chem.* **1982**, *86*, 982.
- (24) Speedy, R. J. *J. Phys. Chem.* **1987**, *91*, 3354.
- (25) Eberhart, J. G.; Schnyders, H. C. *J. Phys. Chem.* **1973**, *77*, 2730.
- (26) Hareng, M.; Leblond, J. J. *Chem. Phys.* **1980**, *72*, 622.
- (27) Truskett, T. M.; Debenedetti, P. G.; Sastry, S.; Torquato, S. *J. Chem. Phys.* **1999**, *111*, 2647.
- (28) Leyendekkers, J. V.; Hunter, R. J. *J. Chem. Phys.* **1985**, *82*, 1440.
- (29) Hare, D. E.; Sorensen, C. M. *J. Chem. Phys.* **1986**, *84*, 5085.
- (30) Postorino, P.; Tromp, R. H.; Ricci, M.-A.; Soper, A. K.; Neilson, G. W. *Nature* **1993**, *366*, 668.
- (31) Tromp, R. H.; Postorino, P.; Neilson, G. W.; Ricci, M. A.; Soper, A. K. *J. Chem. Phys.* **1994**, *101*, 6210.

- (32) Yamanaka, K.; Yamaguchi, T.; Wakita, H. *J. Chem. Phys.* **1994**, *101*, 9830.
- (33) Mountain, R. D. *J. Chem. Phys.* **1995**, *103*, 3084.
- (34) Jedlovsky, P.; Vallauri, R. *J. Chem. Phys.* **1996**, *105*, 2391.
- (35) Bellissent-Funel, M.-C.; Tassaing, T.; Zhao, H.; Beysens, D.; Guillot, B.; Guissani, Y. *J. Chem. Phys.* **1997**, *107*, 2942.
- (36) Chialvo, A. A.; Cummings, P. T.; Simonson, J. M.; Mesmer, R. E.; Cochran, H. D. *Ind. Eng. Chem. Res.* **1988**, *27*, 3021.
- (37) Soper, A. K.; Bruni, F.; Ricci, M. A. *J. Chem. Phys.* **1997**, *106*, 247.
- (38) Khan, A. *J. Chem. Phys.* **1999**, *110*, 11884.
- (39) Kell, G. *J. Chem. Eng. Data* **1975**, *20*, 97, Table 3.
- (40) Schufle, J. A.; Venugopalan, M. *J. Geophys. Res.* **1967**, *72* (12), 3271.
- (41) Schufle, J. A. *Chem. Ind.* **1965**, 690.
- (42) Hare, D. E.; Sorensen, C. M. *J. Chem. Phys.* **1987**, *87*, 4840.
- (43) Pauling, L. *Nature of Chemical Bond*; Cornell University Press: Ithaca, New York, 1948.
- (44) Haggis, G. H.; Buchanan, T. J. *J. Chem. Phys.* **1952**, *20*, 1452.
- (45) Ohmine, I. *J. Phys. Chem.* **1995**, *99*, 6767.
- (46) Luck, W. A. P. in *Water, A Comprehensive Treatise*; F. Franks, Ed., Plenum: New York, 1973; Vol. 2, Ch 4.
- (47) Chen, S.-H.; Teixeira, J. *Adv. Chem. Phys.* **1986**, *64*, p 31.
- (48) Gorbaty, Y. E.; Kalinichev, A. G. *J. Phys. Chem.* **1995**, *99*, 5336.
- (49) Soper, A. K.; Ricci, M. A. *Phys. Rev. Lett.* **2000**, *84*, 2881.
- (50) Khan, A. *J. Phys. Chem.* **1995**, *99*, 12450.
- (51) Khan, A. *Chem. Phys. Lett.* **1996**, *253*, 299.
- (52) Khan, A. *Chem. Phys. Lett.* **1996**, *258*, 574.
- (53) Khan, A. *J. Chem. Phys.* **1997**, *106*, 5537.
- (54) Guissani, Y.; Guillot, B. *J. Chem. Phys.* **1993**, *98*, 8221.
- (55) Lonsdale, D. K. *Proc. R. Soc. A* **1951**, *205*, 193.